UDK 629.5.017.22:7.021.5 ISSN 1580-2949
Original scientific article/Izvirni znanstveni članek MTAEC9, 58(2)193(2024)

THREE-DIMENSIONAL MODEL OF EQUIVALENT ROLL GAP OF CVC MILL UNDER CONDITIONS OF ROLL CROSSING AND NO LOAD

TRIDIMENZIONALNI MODEL EKVIVALENTNE VALJARSKE REŽE CVC VALJARNE V POGOJIH BREZ OBREMENITVE IN KRIŽANJA VALJEV

Xiaoxin Ma[1*], Peisen Yuan[2], Fuyi Li[2], Jiang Ji[3]

[1]Faculty of Mechanical Engineering, Hebei University of Architecture, Zhangjiakou, Hebei, China
[2]College of Mechanical and Vehicle Engineering, Taiyuan University of Technology, Taiyuan, Shanxi, China
[3]China National Heavy Machinery Research Institute Co., Ltd, Xi'an, Shaanxi, 710032, China

Prejem rokopisa – received: 2023-11-14; sprejem za objavo – accepted for publication: 2024-02-07

doi:10.17222/mit.2023.1047

Traditional roll technologies focus solely on the contour of the roll gap at the outlet under ideal conditions. However, upon roll crossing, the three-dimensional distribution of the deformation zone becomes asymmetrical, leading to an adverse impact on the rolling pressure in the deformation zone. To study the screw-down load deviation of plate mills, it is necessary to accurately calculate the equivalent three-dimensional roll gap in the deformation zone under roll-crossing conditions. In this paper a model for calculating the equivalent three-dimensional roll gap under the conditions of roll crossing and no load was established based on the method of the coordinate nonlinear transformation of the spatial rectangular coordinate system. Based on this model, the influences of roll-crossing angles and translation parameters on the symmetry of the equivalent three-dimensional roll gap were analyzed. The distribution of the three-dimensional equivalent roll gap was calculated with different roll lengths, roll radii, and the roll gap's nominal thickness. The intuitive contour map reveals that under the same condition of crossing angle and translation parameters, the larger the roll length and roll radii and the smaller the roll gap's nominal thickness are, the greater the influence of the roll crossing on the asymmetrical distribution of roll gap is. It put forward a quantitative calculation method for evaluating the symmetrical distribution of the roll gap, and the calculation results can provide the equivalent roll profile for the roll-deformation model.

Keywords: roll crossing, nonlinear transformation, equivalent three-dimensional roll gap, asymmetrical distribution

Tradicionalne valjarniške tehnologije se osredotočajo predvsem na konturo reže v idealnih pogojih na izhodu med valjema. Vendar pa na križišču valjev nastane nesimetrična tridimenzionalna deformacija, kar posledično vodi do neželjenega oziroma neugodnega vpliva v coni deformacije. Zato, da bi lahko študirali nihanje obremenitve zategnitve plošč valjev so avtorji natančno izračunali ekvivalentno tridimenzionalno režo med valji vconi deformacije pri pogojih križanja valjev. V tem članku avtorji opisujejo model za izračun ekvivalentne tridimenzionalne valjarske reževpogojih križanja valjev brez obremenitve. Metoda temelji na koordinatni nelinearni transformaciji prostorskega pravokotnega koordinatnega sistema. Na osnovi tega modela so avtorji analizirali vpliv kotov križanja valjev in translacijskih parametrov na simetrijo ekvivalentne tridimenzionalne valjarske reže. Izračunali so porazdelitev tridimenzionalne ekvivalentne valjarske reže za različne dolžine valjev, polmera valjev in nominalno debelino reže. Ugotovljena mapa konture je pokazala da je, pri enakih pogojih kota križanja in enakih translacijskih parametrih, vpliv križanja večji čim večjaje dolžina, čim večji je premer valjev in čim manjša je nominalna debelina reže med valjema. To je v nadaljevanju omogočilo izdelati kvantitativno računsko metodo za ovrednotenje simetrične porazdelitve valjarske reže. Rezultati izračuna pa so lahko podlaga za ekvivalentni profil valjev v modelu za deformacijo valjev.

Ključne besede: križanje valjev, nelinearna transformacija, ekvivalentna tridimenzionalna reža med valjema, nesimetrična porazdelitev

1 INTRODUCTION

Roll technology is the most active and effective shape-control technology. Various advanced techniques have been designed for different purposes, such as the paired crossed (PC) rolling mill,[1] the continuously variable crown (CVC) roll profile technology,[2] the asymmetry self-compensating work roll (ASR) technology,[3] the large concave roll (LCR) technology,[4] the edge variable crown (EVC) roll technology,[5] the SmartCrown roll technology,[6] the SVT roll technology,[7] and linearly variable crown (LVC) roll technology.[8] The core of new roll technologies is to change the roll gap by crossing or shifting the upper and lower work rolls (WRs). The roll gap is an important factor that affects both the strip profile and the distribution of the rolling pressure.

Ideally, the strip profile is mainly affected by the two-dimensional (2D) profile of the outlet at the deformation zone. To realize precise control of the strip profile, many studies are about the calculation of the equivalent 2D roll gap of the outlet of the deformation zone. The equivalent roll crown of the cubic CVC roll curve was discussed in depth.[9] It showed that the equivalent roll crown, considering the width of the strip, is a linear function of both the amount of roll shafting and the roll length, and is also a quadratic function of the strip width. Li Hongbo et al.[10] designed a quintic CVC roll profile, which can equalize the quadratic crown control capabil-

*Corresponding author's e-mail:
mxxwzgz@163.com (Xiaoxin Ma)

ity for both wide and thin strips and show excellent control capability for both the quadratic and the quartic crowns for the ultra-wide strip. F. Schausberger et al.[11] put forward a continuum-mechanics approach to systematically derive the longitudinal contour evolution of the plate based on the input and output thickness. The PC technology can achieve large adjustment domains for the strip crown. The equivalent roll-gap crown model after roll crossing is very important for strip crown control, and the calculation models after roll symmetrically and asymmetrically crossing were established based on the assumption that the cross sections of the rolls were circular or ellipse.[12–14] The thermal and wear contours of the online work roll are also the main factors that influence the strip profile. Therefore, online prediction models for the 2D roll gap are also research cores. A computer model based on the finite-difference method was applied to predict the model for the work-roll thermal profile.[15] R. Servin Castañeda et al.[16] put forward a roll-wear prediction model of a hot strip mill. It mainly considered the influence of the Hertzian pressure distribution and the mechanical contact between two cylinders with parallel axes.[17] X. D. Wang et al.[18] put forward a predictive calculation model for the work roll comprehensive contour, which is the superposition of the initial, thermal, and wear contours of work rolls.

The above studies on the strip profile only concerned the 2D roll gap at the outlet of the deformation zone. The shape change of the roll gap has little effect on the load distribution under the symmetry condition, thus, the influence is neglected. However, in the case of asymmetry, the impact of the roll gap on the rolling load is severe. The applications of the PC rolling mill and the CVC roll contour have led to many load problems, especially the thrust load and the screw-down load deviation. Both the great deviation of the screw-down load and the roll damage frequently occurred in the 1580-mm PC mill of Baosteel. The main reason for the dynamic screw-down load deviation was identified as the axial force resulting from roll crossing.[19] In addition, the problems of thrust bearing burning and short service life which frequently arose in a 2350 aluminum foil mill were also considered to be caused by the great thrust force due to the roll crossing.[20] The reasons for those problems definitely point to the stability of the rolls or roll crossing. Aiming at roll crossing, Sheng et al.[21–23] firstly put forward new theories of the roll spiral precession, the dynamic roll crossing, and the microscale dimension behavior. They pointed out that the mechanism of setting eccentricity between rolls was adverse to the roll stability. It was prone to cause dynamic roll crossing behavior and eventually led to the great axial force, which is the main reason for the bearing shortened longevity and burn damage. To this end, the mechanical statically determinate structure of rolling mills was proposed to solve the problem. However, those investigations not only did not establish the effect evaluation of the roll crossing on the rolling load, but also did not give an explanation for the deviation of the screw-down load. The asymmetrial deformation zone is one of the characteristics of asynchronous rolling.[24–26] However, the roll gap of asynchronous rolling is asymmetric regarding up and down rather than about left and right along the roll barrel. The asynchronous rolling process is mainly affected by different circumferential velocities or different work-roll radii.

According to the above analyses, the present studies aim only at the equivalent 2D roll gap at the outlet of the deformation zone. There is little research on the equivalent three-dimensional (3D) roll gap under roll-crossing conditions, which has a vital influence on the rolling load distribution along the deformation zone. The great screw-down load deviation has occurred in a 5000-mm heavy plate mill, which can reach 200 t to 400 t, accounting for 3–6 % of the total rolling force. It seriously harms the mill equipment and leads to significant bent defects for heavy plates. The axial force of the backup roll (BUR), which would generate an additional moment on the screw-down, is considered one of the main reasons for the screw-down load deviation.[27] Furthermore, another important factor for the screw-down load deviation is the distribution of the rolling pressure, especially under roll-crossing conditions. The asymmetrical distribution of the deformation zone after roll crossing is a direct reason for the asymmetrical distribution of the rolling pressure in the deformation zone. It is obviously one-sided to apply the 2-D equivalent roll gap at the outlet of the deformation zone to evaluate the whole roll gap in the deformation zone after roll crossing. In particular, the work roll is the CVC profile, and the distribution of the deformation zone is nonlinear after roll crossing, which means that the equivalent roll contours from the inlet to the outlet of the deformation zone are not parallel. Therefore, one of the key issues for the research on screw-down load deviation is to establish the equivalent 3D roll gap in the deformation zone. In this paper, the 3D distribution of both the upper and lower roll contours after roll crossing is established based on the coordinate nonlinear transformation of the spatial rectilinear coordinate system. Finally, the 3D roll gap is reconstructed without load conditions, and intuitive contour maps are used to reveal the asymmetrical distribution of the deformation zone.

2 NONLINEAR TRANSFORMATION MODEL OF ROLL CROSSING

2.1 Roll crossing modeling principle

Reconstruction of the equivalent 3D roll gap under the conditions of roll crossing and no load needs to establish the 3D roll model. **Figure 1** is a sketch map of the CVC WR under roll-crossing conditions. The Y_0-axis of the spatial rectangular coordinate system O_0–$X_0Y_0Z_0$ is the rotatory central line of the lower CVC WR, and the

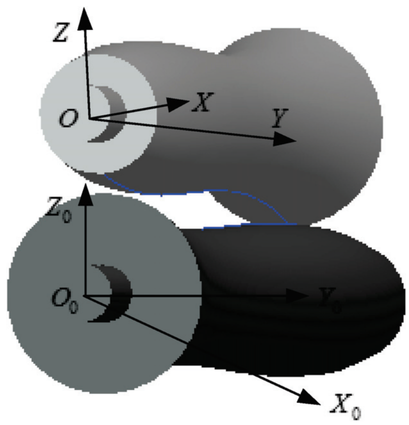

Figure 1: Sketch map of upper and lower CVC work rolls under the condition of roll crossing

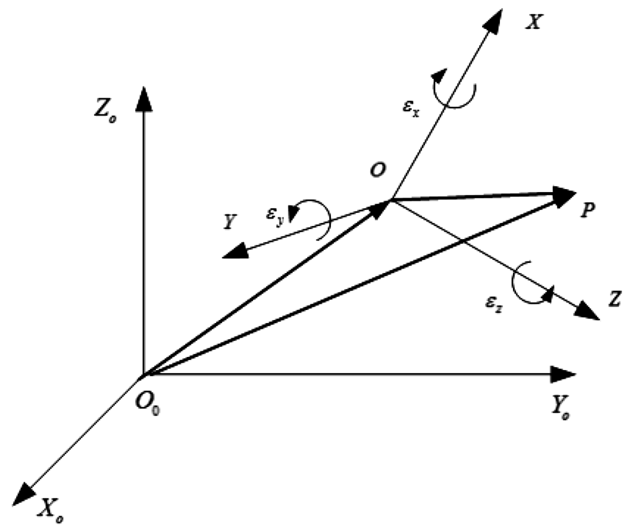

Figure 2: Schematic of the transformation of the spatial rectangular coordinate system

vertical direction is the Z_0-axis, the X_0-axis is perpendicular to the plane O_0–Y_0Z_0. Under the ideal condition, the upper and lower WR axes are parallel. When the upper and lower WRs are crossing, the rotation axes of the upper and lower WR occur with a spatial intersection, resulting in the rotation of the local spatial rectangular coordinate system of the upper roll *O–XYZ*. The coordinate transformation formula of two different spatial coordinate systems is established to solve the equivalent 3-D roll gap under the conditions of roll crossing and no load.

2.2 Coordinate nonlinear transformation model of space rectangular coordinate system

Figure 2 is a schematic diagram of the transformation of a spatial rectangular coordinate system. $\boldsymbol{O_0P}$ is a vector in the absolute spatial rectangular coordinate system O_0–$X_0Y_0Z_0$. $\boldsymbol{O_0P}$ is a vector in the local spatial rectangular coordinate system *O–XYZ*. $\boldsymbol{O_0O}$ is the vector from the origin of the absolute spatial rectangular coordinate system O_0–$X_0Y_0Z_0$ to the origin of the local spatial rectangular coordinate system *O–XYZ*. The coordinates of *O* in the coordinate system O_0–$X_0Y_0Z_0$ are (X_0^{T}, Y_0^{T}, Z_0^{T}), i.e., they are the translation parameters of the rectangular coordinate system O_0–$X_0Y_0Z_0$ to the rectangular coordinate system *O–XYZ*. As a result of the rotation of the coordinate system, there are three rotation-angle parameters ε_x, ε_y, ε_z, which the axes of the local coordinate system *O–XYZ* are parallel to the axes of the absolute coordinate system O_0–$X_0Y_0Z_0$ after rotation. In addition, the unit vector of two coordinate systems can be different, and the unit dimension of the original absolute rectangular coordinate system O_0–$X_0Y_0Z_0$ is 1, while the scale of the unit of the local rectangular coordinate system *O–XYZ* increases K_1.

The coordinates of a point *P* in the coordinate system O_0–$X_0Y_0Z_0$ are (X_0^i, Y_0^j, Z_0^k), and in the coordinate system *O–XYZ* are (X^i, Y^j, Z^k). The relationship between them is as follows:[28]

$$\begin{bmatrix} X_0^i \\ Y_0^j \\ Z_0^k \end{bmatrix} = \begin{bmatrix} X_0^{\mathrm{T}} \\ Y_0^{\mathrm{T}} \\ Z_0^{\mathrm{T}} \end{bmatrix} + (1+K_1)\boldsymbol{R} \begin{bmatrix} X^i \\ Y^j \\ Z^k \end{bmatrix} \tag{1}$$

$$\boldsymbol{R}_x(\varepsilon_x) = \begin{bmatrix} 1 & 0 & 0 \\ 0 & \cos\varepsilon_x & -\sin\varepsilon_x \\ 0 & \sin\varepsilon_x & \cos\varepsilon_x \end{bmatrix}, \quad \boldsymbol{R}_y(\varepsilon_y) = \begin{bmatrix} \cos\varepsilon_y & 0 & \sin\varepsilon_y \\ 0 & 1 & 0 \\ -\sin\varepsilon_y & 0 & \cos\varepsilon_y \end{bmatrix}, \quad \boldsymbol{R}_z(\varepsilon_z) = \begin{bmatrix} \cos\varepsilon_z & -\sin\varepsilon_z & 0 \\ \sin\varepsilon_z & \cos\varepsilon_z & 0 \\ 0 & 0 & 1 \end{bmatrix}$$

$$\boldsymbol{R} = \begin{bmatrix} \cos(\varepsilon_y)\cos(\varepsilon_z) & \cos(\varepsilon_z)\sin(\varepsilon_y)\sin(\varepsilon_x) - \cos(\varepsilon_x)\sin(\varepsilon_z) & \cos(\varepsilon_x)\sin(\varepsilon_y)\cos(\varepsilon_z) + \sin(\varepsilon_x)\sin(\varepsilon_z) \\ \cos(\varepsilon_y)\sin(\varepsilon_z) & \sin(\varepsilon_x)\sin(\varepsilon_y)\sin(\varepsilon_z) + \cos(\varepsilon_x)\cos(\varepsilon_z) & \cos(\varepsilon_x)\sin(\varepsilon_y)\sin(\varepsilon_z) - \cos(\varepsilon_z)\sin(\varepsilon_x) \\ -\sin(\varepsilon_y) & \cos(\varepsilon_y)\sin(\varepsilon_x) & \cos(\varepsilon_x)\cos(\varepsilon_y) \end{bmatrix} \tag{2}$$

Where $\boldsymbol{R} = \boldsymbol{R}_z(\varepsilon_z)\boldsymbol{R}_y(\varepsilon_y)\boldsymbol{R}_x(\varepsilon_x)$,

As a result of the roll flattening between the BUR and the WR, the setting of the offset distance becomes invalid, leading to a failure of the horizontal force.[18] Additionally, the initial gap and the extent of the wear between the roll bearing chocks and the mill housings are inevitable. In particular, the screw-down stroke of the heavy plate rolling mill is large and the AGC frequently and dynamically adjusts so that the amount of wear and the gap are relatively large. All of those will lead to the roll crossing. However, the offset distance, the initial gap and the wear between the bearing chock and housing are relatively small compared with the roll length and the radius of the heavy-plate rolling mill. The crossing angle of the upper and lower WRs is generally less than 0.5°. Therefore, the values of ε_x, ε_y, and ε_z can be treated as minute quantities. According to the Taylor formula, the $\sin(\varepsilon)$ and $\cos(\varepsilon)$ can be expanded to a power series of ε, which can be expressed as follows:

$$\sin(\varepsilon) = \varepsilon - \frac{\varepsilon^3}{3!} + \frac{\varepsilon^5}{5!} + \ldots + \frac{(-1)^{n-1}\varepsilon^{2n-1}}{(2n-1)!} + \ldots \tag{3}$$

$$\cos(\varepsilon) = 1 - \frac{\varepsilon^2}{2!} + \frac{\varepsilon^4}{4!} + \ldots + \frac{(-1)^{n}\varepsilon^{2n}}{(2n)!} + \ldots \tag{4}$$

From Equations (3) and (4), as well as the derivative relationship of Equation (2), and ignoring the higher-order infinitesimal that is more than the quadratic term of the ε, the following equations can be obtained:

$$\boldsymbol{R} = \begin{bmatrix} 1-\dfrac{\varepsilon_y^2+\varepsilon_z^2}{2} & \varepsilon_x\varepsilon_y-\varepsilon_z & \varepsilon_x\varepsilon_z+\varepsilon_y \\ \varepsilon_z & 1-\dfrac{\varepsilon_x^2+\varepsilon_z^2}{2} & \varepsilon_y\varepsilon_z-\varepsilon_x \\ -\varepsilon_y & \varepsilon_x & 1-\dfrac{\varepsilon_x^2+\varepsilon_y^2}{2} \end{bmatrix} \tag{5}$$

From Equations (1) and (5), the relationship between the two coordinate systems of the upper and lower WR can be established:

$$\begin{bmatrix} X_0^i \\ Y_0^j \\ Z_0^k \end{bmatrix} \approx \begin{bmatrix} X_0^{\mathrm{T}} + (1+K_1)\left[\left(1-\dfrac{\varepsilon_y^2+\varepsilon_z^2}{2}\right)X^i + (\varepsilon_x\varepsilon_y-\varepsilon_z)Y^j + (\varepsilon_x\varepsilon_z+\varepsilon_y)Z^k\right] \\ Y_0^{\mathrm{T}} + (1+K_1)\left[\varepsilon_z X^i + \left(1-\dfrac{\varepsilon_x^2+\varepsilon_z^2}{2}\right)Y^j + (\varepsilon_y\varepsilon_z-\varepsilon_x)Z^k\right] \\ Z_0^{\mathrm{T}} + (1+K_1)\left[-\varepsilon_y X^i + \varepsilon_x Y^j + \left(1+\dfrac{\varepsilon_x^2+\varepsilon_y^2}{2}\right)Z^k\right] \end{bmatrix} \tag{6}$$

The position and direction of the local coordinate system of the upper and lower WRs change before and after the roll crossing, while the scale factor of the local coordinate system will not change, i.e., $K_1 = 0$. The translation parameters from the absolute spatial rectangular coordinate system of the lower roll O_0–$X_0Y_0Z_0$ to the local spatial rectangular coordinate system of the upper roll O–XYZ can be determined by the offset distance of the roll and the crossing angle. If the rotation angle of the three directions is given, the equivalent roll gap in the deformation zone can be obtained.

3 MODEL OF EQUIVALENT 3D ROLL GAP UNDER ROLL-CROSSING CONDITIONS

In the spatial rectangular coordinate system O_0–$X_0Y_0Z_0$, the equation of the lower roll is expressed as:

$$\begin{aligned} & x^2 + z^2 = r^2 \\ & r = R_{\mathrm{w}} + a_1(l_{\mathrm{w}} - (y - s_{\mathrm{w}}) + e) + \\ & + a_2(l_{\mathrm{w}} - (y - s_{\mathrm{w}}) + e)^2 + a_3(l_{\mathrm{w}} - (y - s_{\mathrm{w}}) + e)^3 \end{aligned} \tag{7}$$

where $y \in [s_{\mathrm{w}}, s_{\mathrm{w}} + l_{\mathrm{w}}]$; s_{w} is the distance from the center line of the housing to the end of the WRs; l_{w} is the length of the WRs; e is the shifting displacement of the WRs; R_{w} is the nominal radius of the WRs; a_1, a_2, and a_3 are the coefficients of the cubic curve of the contour of the CVC WR.

According to Equations (1) and (6), the transformation relationship between the spatial rectangular coordinate system O–XYZ and the spatial rectangular coordinate system O_0–$X_0Y_0Z_0$ is obtained, and the upper-roll equation in the spatial rectangular coordinate system O_0–$X_0Y_0Z_0$ is:

$$\begin{aligned} & (Z_0^{\mathrm{T}} + \varepsilon_y A - \varepsilon_x B + zC)^2 + (A)^2 = \Big\{R_{\mathrm{w}} + a_1\big[l_{\mathrm{w}} + s_{\mathrm{w}} + e - B\big] + \\ & + a_2\big[l_{\mathrm{w}} + s_{\mathrm{w}} + e - B\big]^2 + a_3\big[l_{\mathrm{w}} + s_{\mathrm{w}} + e - B\big]^3\Big\}^2 \end{aligned} \tag{8}$$

$$A = X_0^T - x\left(\frac{\varepsilon_y^2+\varepsilon_z^2}{2} - 1\right) - y(\varepsilon_z - \varepsilon_x\varepsilon_y) + z(\varepsilon_y + \varepsilon_x\varepsilon_z)$$

$$\begin{aligned} B = {} & Y_0^{\mathrm{T}} + \varepsilon_z\left\{X_0^{\mathrm{T}} - x\left(\frac{\varepsilon_y^2+\varepsilon_z^2}{2} - 1\right) - y(\varepsilon_z - \varepsilon_x\varepsilon_y) + \right. \\ & \left. + z(\varepsilon_y + \varepsilon_x\varepsilon_z)\right\} - y\left(\frac{\varepsilon_x^2+\varepsilon_z^2}{2} - 1\right) - z(\varepsilon_x - \varepsilon_y\varepsilon_z) \end{aligned}$$

$$C = \left(\frac{\varepsilon_x^2+\varepsilon_y^2}{2} - 1\right)$$

$$x = l_x \tag{9}$$

where $l_x \in [0, l]$; l is the projection length of the contact arc of the deformation zone. Combining Equations (7), (8), and (9), the following equivalent equation of the upper and lower roll curves at the position $x = l_x$ in the deformation zone can be obtained:

$$\begin{aligned} & f_x(y,z)\big|_{x=l_x,\ (R_{\mathrm{w}}-\delta)\le z\le(R_{\mathrm{w}}+\delta)} \\ & f_s(y,z)\big|_{x=l_x,\ R_{\mathrm{w}}<z\le Z_0^{\mathrm{T}}} \end{aligned} \tag{10}$$

where δ is the difference between the maximum and minimum CVC roll radii. Then the distribution of the equivalent roll gap in the deformation zone is obtained:

$$h(y,z) = f_{\mathrm{s}}(y,z) - f_x(y,z) \quad (x{=}l_x) \tag{11}$$

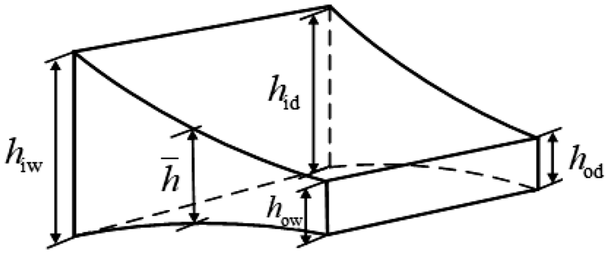

Figure 3: Sketch map of the roll gap

To facilitate the quantitative evaluation of the asymmetry of the 3D roll gap in the deformation zone, the asymmetry degree of the roll gap is defined as:

$$A_{ag} = \frac{1}{2}\left(\frac{\max(h_{iw}, h_{id})}{\min(h_{iw}, h_{id})} + \frac{\max(h_{ow}, h_{od})}{\min(h_{ow}, h_{od})}\right) \tag{12}$$

Further, the relative asymmetry of the roll gap can be obtained:

$$A_{rg} = \frac{\Delta h}{\bar{h}} A_{ag} \tag{13}$$

where h_{iw} and h_{id}, as shown in **Figure 3**, are the thicknesses at the working side and the driving side of the inlet of the roll gap, respectively. h_{ow} and h_{od} are the thicknesses at the working side and the driving side of the outlet of the roll gap, respectively. The thickness reduction and the average thickness of the roll gap can be expressed as:

$$\Delta h = \frac{(h_{iw} + h_{id}) - (h_{ow} + h_{od})}{2} \tag{14}$$

$$\bar{h} = \frac{(h_{il} + h_{ir}) + (h_{ol} + h_{or})}{4} \tag{15}$$

Both values of A_{ag} and A_{rg} represent the asymmetry of the roll gap. The closer the value of A_{ag} to 1, the more symmetrical the roll gap, and the less the value of A_{rg}, the smaller the impact of roll crossing.

4 EFFECT OF ROLL CROSSING ON THE SYMMETRY OF THE EQUIVALENT 3D ROLL GAP OF CVC ROLLING MILLS

Many factors will lead to roll crossing, such as the gap between the bearing chocks of the WR and the BUR and the mill stand housing, the symmetry of the mill housing installation and manufacture, the oil-film thickness of the BUR bearing, the additional moment from the transmission shaft acting on the WR, the roll eccentricity between the rolls, the roll contour, and so on. The size of the intersection angle can only be determined by main factors. Under the no-load condition, the influence factors of the equivalent 3D roll gap shape include the three rotation parameters, the three translation parameters, the WR radius and the length, and the roll gap's nominal thickness. The equipment parameters and clearance parameters of a 5000-mm-wide and heavy plate rolling mill and a 1580-mm hot-rolling mill are shown in **Table 1**. The parameters of the two CVC roll mills were used in the model calculation, and the crossing angles of the upper and lower WRs were estimated according to those parameters.

Table 1: Parameters of 5000 mm and 1580 mm CVC rolling mill

Rolling mill type	5000-mm mill	1580-mm mill
WR radius R_w/mm	600	400
WR barrel length l_w/mm	5300	1580
Distance between both screw-downs l_a/mm	7000	2760
Eccentricity between rolls between center lines of WR and BUR Δ/mm	10	10
Gap between WR chock and housing $\Delta\delta_w$/mm	1–4	1–4
Gap between BUR chock and housing δ_b/mm	3–8	3–5

Equations (7) and (8) of the WR are binary cubic functions about y and z, and the final derived Equation

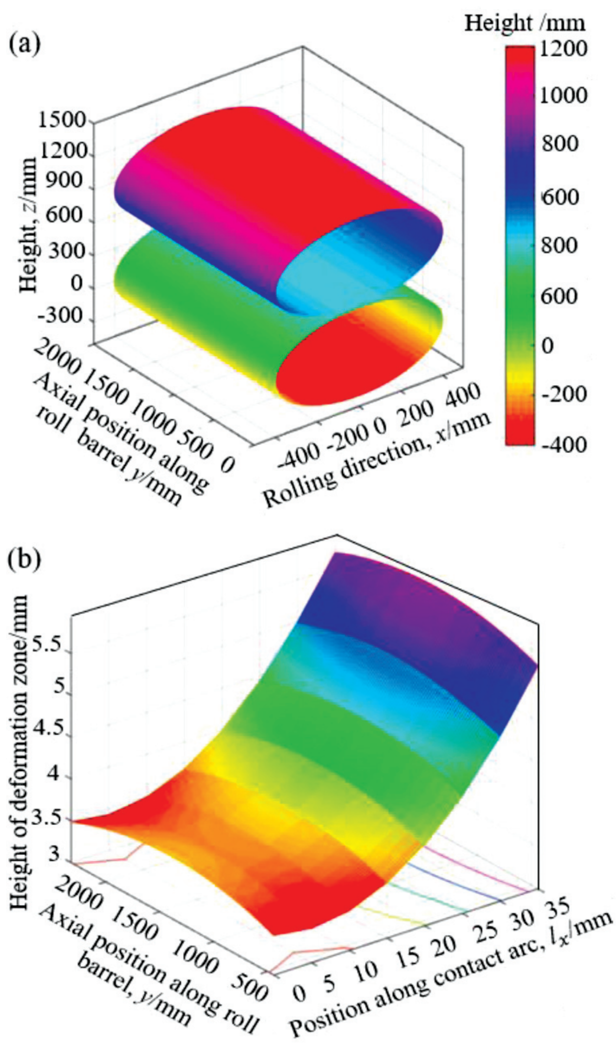

Figure 4: 3D work rolls and equivalent roll gap: a) work rolls, b) equivalent roll gap

Table 2: Rotation parameters and translation parameters in simulated instances

	ε_x	ε_y	ε_z	X_0^{T}/mm	Y_0^{T}/mm	Z_0^{T}/mm
Example 1	0.0005	0	0	10	1	$2R_{\mathrm{w}}$ + 4
Example 2	0	0.0005	0	10	1	$2R_{\mathrm{w}}$ + 4
Example 3	0	0	0.003	10	1	$2R_{\mathrm{w}}$ + 4

(11) of the equivalent roll gap is an implicit function, it will be extremely difficult to change the implicit function into the explicit form. It is recommended to use some mathematical calculation tools to solve this implicit function. This study established a calculation program of equivalent 3D roll gaps using MATLAB software. Taking the parameter of 1580-mm CVC work rolls as an example, the results of the 3D distribution of the work rolls and the equivalent roll gap obtained are shown in **Figures 4a** and **4b**, respectively.

The crossing angle ε_z means that the upper WR rotates around the Z_0 axis in the horizontal plane O_0–X_0Y_0. It is mainly affected by the gaps δ_{w}, δ_{b}, between the bearing blocks of both the WRs and the BURs and the mill housing. The rolling distance of the BUR is large, and the roll change period is so long that the gap between the BUR bearing chocks and the mill housing is larger than that between the WR bearing chocks and the mill housing. Hot-rolling mills, especially the heavy-plate rolling mill, are characterized by the large opening degree of roll gap, the large screw-down stroke, and the frequent movement of hydraulic AGC, it is very likely to cause roll crossing. In the case of serious wear, the gap between the BUR bearing chock and stand housing was 1.2 times the technical requirement. Furthermore, if the function of the eccentricity between rolls Δ is failure, the crossing angle is about:

$$\varepsilon_{z\max} = \frac{2(\delta_{\mathrm{w}} + 1.2\delta_{\mathrm{b}}) + \Delta}{l_{\mathrm{a}}} \tag{16}$$

The crossing angle ε_y means that the upper WR rotates around the Y_0 axis in the vertical plane O_0–X_0Z_0. It is due to the rotation of the CVC roll contour, which has no effect on the 3D roll gap. The crossing angle ε_x means that the upper WR tilts around the X_0 axis in the vertical plane O_0–Y_0Z_0. It is mainly affected by the zero adjustment of the roll gap, the vertical tilting of the WR, the horizontal crossing angle, and the symmetry of the actual grinding roll contour.

To analyze the influence of different crossing angles on the symmetry of the equivalent 3D roll gap, the contour maps of the equivalent roll gap in the deformation zone are shown in the following figures. The longitudinal coordinate is the axial position along the roll barrel, and the horizontal coordinate is the position along the contact arc. The values of the cross angle and translation parameters in the simulation are shown in **Table 2**. The parameters of the rolls used in the simulation adopt the those of the 1580-mm and 5000-mm rolling mills in **Table 1**.

Figure 5 shows contour maps of the equivalent roll gap affected by rotational parameters, namely ε_x, ε_y, and ε_z. and the roll contours in the roll gap from the inlet to the outlet of the deformation zone. Among the three rotation parameters, rotation around the Y_0-axis has no effect on the roll gap, which is consistent with the theoretical analysis and proves the correctness of the model. The absolute asymmetry degrees of the roll gap, A_{ag}, in **Figures 5a** to **5c** are approximately 1.31, 1, and 1.06, respectively. This indicates that rotation around the X_0-axis has the greatest impact on the asymmetry of the roll gap, while rotation around the Z_0-axis has a secondary impact on the roll gap. In fact, a large number of simulation analyses shows that the roll-gap asymmetry develops significantly with the increase of ε_x. The larger the tilt angle ε_x, the greater the influence on the asymmetry degree of roll gap. Even if the tilt angle ε_x is equal to 0.0001, the absolute asymmetry degrees of the roll gap, A_{ag} will reach 1.05, which is roughly equal to that of example 3, and the vertical height difference, $\delta_{\mathrm{h}} = l_{\mathrm{a}}\varepsilon_x$, between the working and driving sides of the 1580-mm rolling mill will reach 0.276 mm at the same time. It is necessary to strictly control the vertical leveling of the roll gap. In **Figure 5d**, the roll contours do not keep parallel from the inlet to the outlet of the deformation zone when the roll axis rotates around the X_0-axis and Z_0-axis, simultaneously. Namely, it is inaccurate that the 2D equivalent roll contour is used to evaluate the entire gap. It causes an error if the rolling force is calculated by using the roll contour at the outlet of the deformation. The thinner the roll gap and the greater the steel deformation resistance, the larger the error.

According to Equations (7), (8), (10), and (11), under the conditions of roll rotation, the equivalent 3D roll gap is a function of the offset position X_0^{T}, Y_0^{T}, Z_0^{T}, x, y, and z. X_0^{T} and Z_0^{T} will alter the relative position of the ends of the upper and lower rolls in the radial direction, and the offset position Y_0^{T} can affect the symmetry of the upper and lower WR profiles after shifting, thereby changing the end position of roll crossing. In fact, the axial direction of the rolls is constrained by the shifting hydraulic cylinder, and the radial direction along the rolling direction is constrained by the mill housing and bearing chocks, thus the offset positions X_0^{T} and Y_0^{T} vary in a limited range. The simulation results indicate that the limited offset positions have little influence on the symmetry of the roll gap. Z_0^{T} is the distance between two work roll axes, which is influenced by both roll radius, R_{w}, and nominal thickness of roll gap, h. The x-coordinate and z-coordinate are distributed along the radial di-

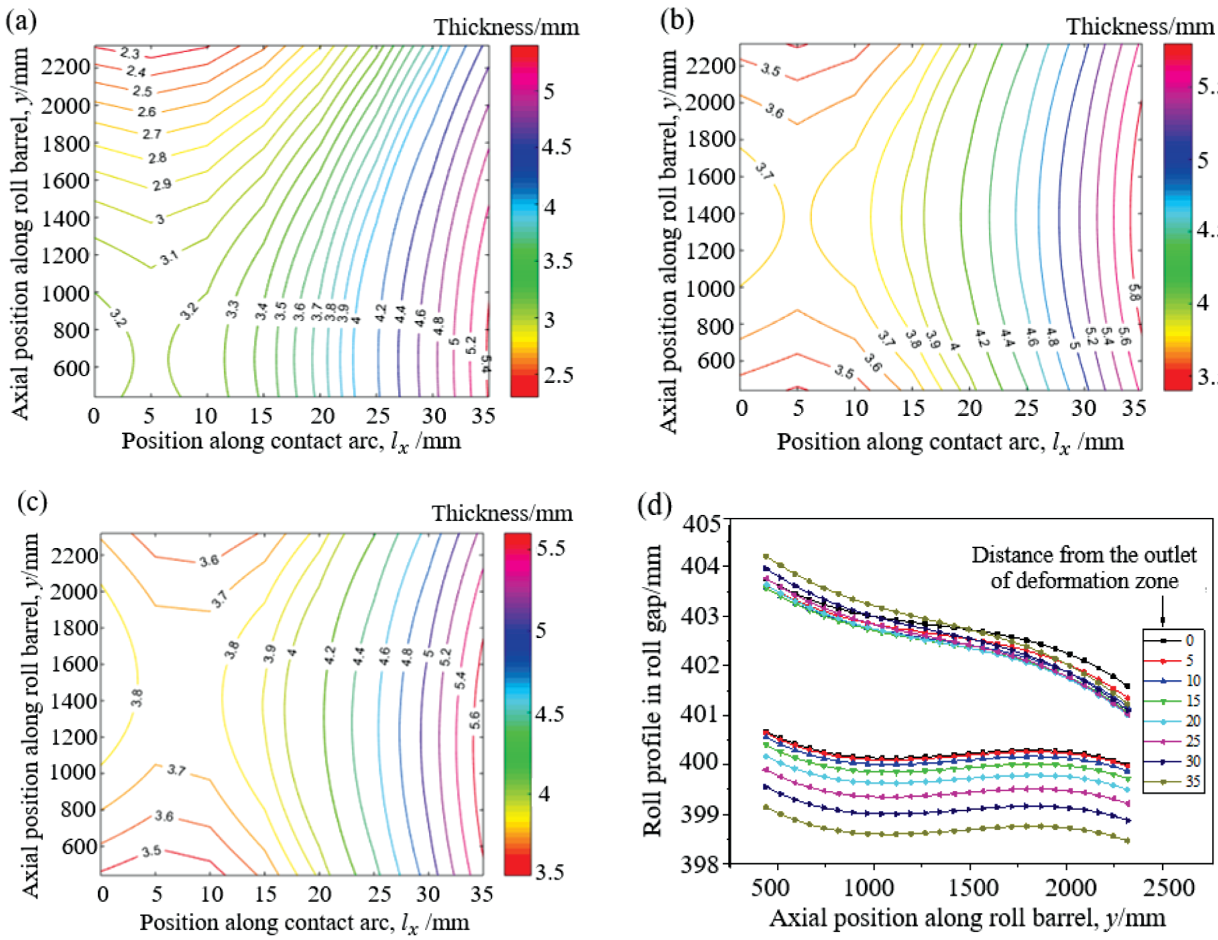

Figure 5: Contour maps of the equivalent roll gaps affected by the rotational parameters and roll contours: a) example 1, b) example 2, c) example 3, d) roll contours in roll gap from inlet to outlet of the deformation zone

rection of the roll barrel, and the *y*-coordinate is distributed along the axial direction, thus the roll barrel length, l_w, and roll radius, R_w, also influence the symmetry of the roll gap under the condition of roll rotation.

To further analyze the influence of the roll barrel length, roll radius, and nominal thickness of the roll gap on the asymmetry of equivalent 3D roll gaps under roll-crossing conditions, simulations were conducted based on the parameters shown in **Table 3**. In examples 4 and 5, both the roll radius and roll gap's nominal thickness of the 5000-mm and 1580-mm rolling mills are 600 mm and 10 mm, the roll-barrel length is variable.

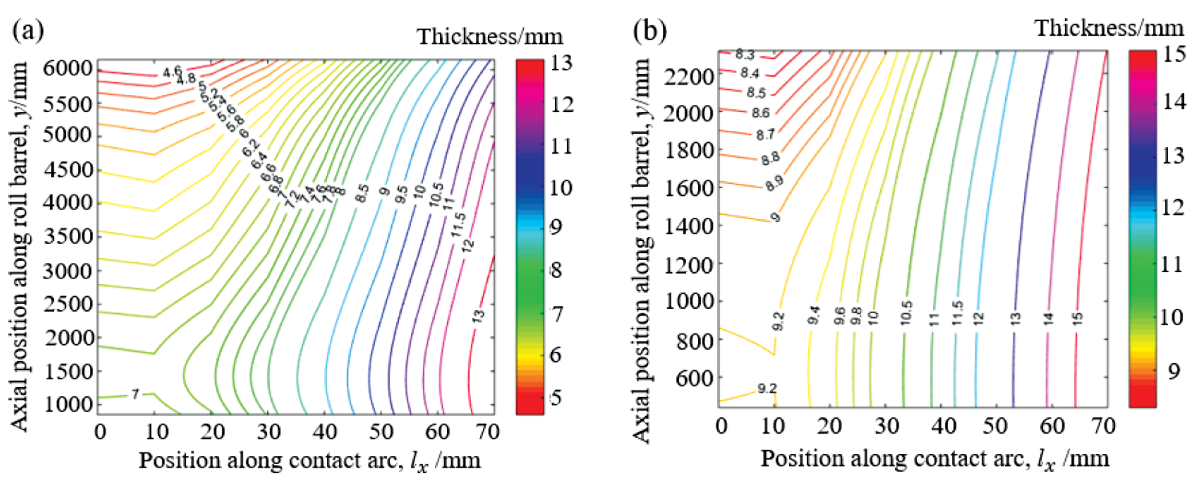

Figure 6: Contour maps of the equivalent roll gaps affected by the work roll-barrel length: a) example 4, b) example 5.

Table 3: Examples of the influence of the work roll barrel length, work roll radius, and roll gap's nominal thickness

Parameters	Example 4	Example 5	Example 6	Example 7	Example 8	Example 9
WR radius R_w/mm	600	600	400	800	400	400
WR barrel length l_w/mm	5300	1580	1580	1580	1580	1580
Roll gap h/mm	10	10	10	10	4	15

Figure 6 shows that the asymmetry degree of the whole equivalent 3D roll gap increases with the roll-barrel length increasing under the condition of the same rotation parameters and translation parameters. The absolute asymmetry degrees of roll gap, A_{ag}, in **Figure 6a** and **6b** are about 1.51 and 1.09, respectively. The result indicates that the longer the roll-barrel length, the greater the influence of the roll crossing on the asymmetry degree of the roll gap. Specifically, when the roll barrel l_w is equal to 5300 mm, the whole equivalent 3D roll gap from the inlet to the outlet exhibits pronounced asymmetry. This means that the wide-plate mill is more susceptible to roll crossing, in terms of the degree of roll-gap asymmetry. In fact, it is precisely because of the roll length of the heavy-plate mill, and the difference in the constraints of both mill housings on roll bearing chocks is particularly prominent. The roll bearing chocks at the operating side bear strong fixed constraints of shifting hydraulic cylinders or thrust plates, while those at the driving side belong to free ends. Furthermore, the roll driving end withstands the disturbance of the additional moment from the main transmission system.[29] Thus, the longer the roll barrel, the easier the rolls to cross, while the asymmetrical roll gap, in turn, is more likely to make the roll crossing. Moreover, **Figure 6** shows that the asymmetry near the outlet is greater than that near the inlet. This indicates that the thinner the roll gap, the greater the influence of roll crossing.

From examples 6 to 7, all the roll-barrel lengths and the roll gap's nominal thicknesses are 1580 mm and 10 mm, respectively, and the influential variable is the roll radius. **Figure 7** shows that the asymmetry degree of the whole equivalent 3D roll gap increases with the roll radius increasing under the condition of the same rotation parameters and translation parameters. However, the absolute asymmetry degrees of roll gap, A_{ag}, in **Figure 7a** and **7b** are about 1.0129 and 1.0178, respectively. Although the asymmetry degree of the equivalent 3D roll gap grows with roll radius increasing, the variation degree is not significant. It can be inferred that the WR radius of the rolling mills has little effect on the asymmetry of the 3D roll gap. For plate-rolling mills, under the condition of constant outlet thickness, large roll radii will cause an increase of the contact arc length in the deformation zone, and the influence of asymmetry three-dimensional roll gap on the distribution of rolling pressure will still be amplified, resulting in screw-down load deviation under the condition of roll crossing.

In examples 8 and 9, all the roll-barrel lengths and the roll radii are 1580 mm and 400 mm, respectively, and the influential variable is the roll gap's nominal thickness. The absolute asymmetry degrees of the roll gap, A_{ag}, in **Figure 8a** and **8b** are about 1.0571 and 1.013, respectively, while the relative asymmetry degrees of the roll gap, A_{rg} are about 0.42 and 0.12, respectively. The results indicate that the asymmetry degree of the whole equivalent 3D roll gap decreases with the roll gap's nominal thickness increasing under the condition of the same rotation parameters and translation parameters. That is, the last pass with a thin gap or the downstream rolling mill, in the matter of the asymmetry degree of roll gap, is much more easily affected by the roll crossing. It indicates that the screw-down load deviation is more likely to occur in the last pass or the downstream rolling mill

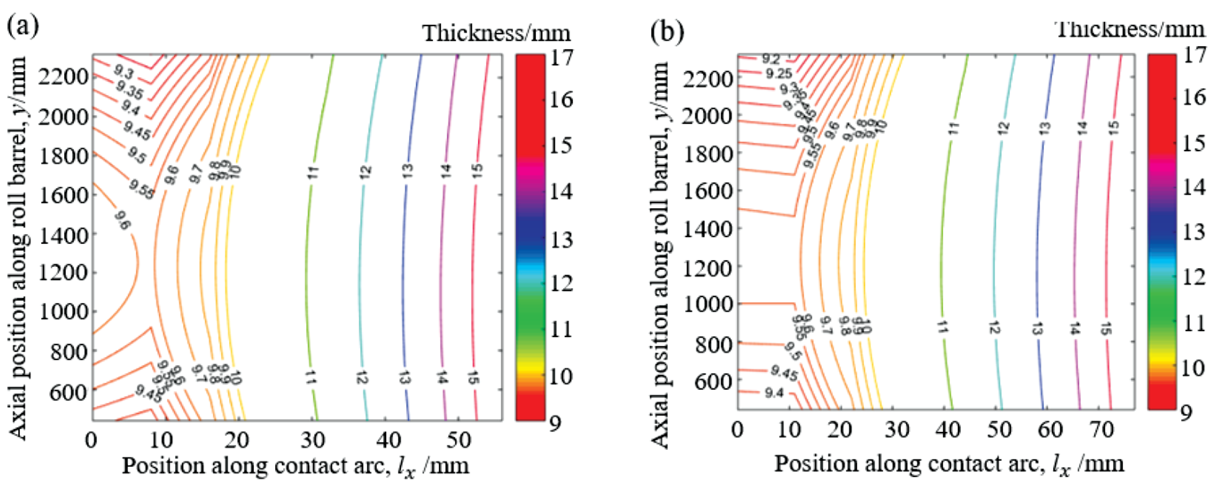

Figure 7: Contour maps of the equivalent roll gaps affected by the work roll radii: a) example 6, b) example 7

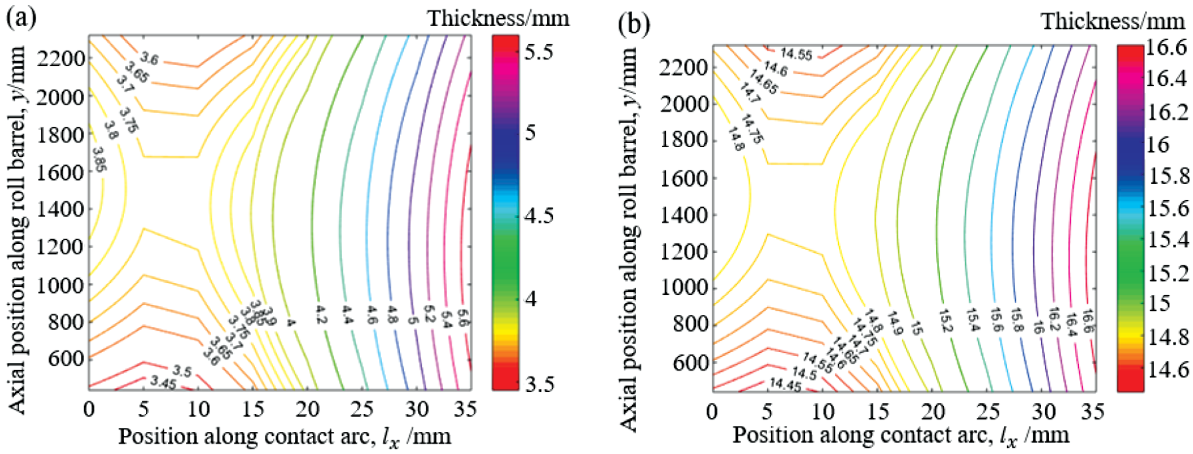

Figure 8: Contour maps of the equivalent roll gaps affected by the roll gap's nominal thickness: a) example 8, b) example 9

under the condition of roll crossing. The problem becomes more significant, especially for the last pass of the heavy-plate rolling mill as the deformation resistance of the plate increases.

According to the influence rules of the roll-barrel length, the roll radius, and the roll gap's nominal thickness on the asymmetry of the roll gap, it can be concluded that the heavy-plate mills are more likely to be affected by roll crossing than ordinary mills, and the great screw-down load deviation is more likely to happen in last pass compared with initial passes, which is consistent with the production practice and reports.[27] For the wide and heavy-plate rolling mill, the rolls would be leveled before rolling, so the rotation of the work rolls around the *x*-axis is controllable. When the rotation angle ε_z of the work rolls around the *z*-axis is less than or equal to 0.004, according to Equation (16), it can be obtained that the sum of clearance and wear extent between the liners of both bearing chocks and mill housing in both the working and driving side should be less than 9 mm.

5 CONCLUSION

To analyze the influence of roll crossing on the asymmetry of roll gap, this study established an equivalent 3D roll-gap model and an evaluation method for asymmetry degree. The influences of roll-crossing parameters on the asymmetry of the 3D roll gap are analyzed. Furthermore, the sensitivity of the work roll-barrel length, roll radius, and nominal thickness of the roll gap to the asymmetry degree of the equivalent 3D roll gap caused by roll crossing is analyzed. Based on the above research, the following conclusions can be drawn:

(1) The 3D model of the upper and lower WR and the equivalent 3D roll-gap model are established based on the coordinate nonlinear transformation model of the spatial rectangular coordinate system. It can be widely applicable to calculate the equivalent 3D roll gap under small crossing angle conditions, and analyze the equivalent roll contours from the inlet to the outlet of the deformation zone for the roll-deformation model.

(2) The equivalent 3D roll gap is affected by the translation parameters (X_0^T, Y_0^T, Z_0^T) and the crossing angle parameters (ε_x, ε_y, ε_z) of the WR. The rotation parameter ε_y does not affect the roll gap. The influence of the rotation parameter ε_x, on the roll gap is much greater than the rotation parameter ε_z. The translation parameters, X_0^T and Y_0^T, vary in a limited range and have little influence on the symmetry of the roll gap.

(3) Under a certain crossing-angle condition, the larger the roll barrel length, the larger the WR radius, and the thinner the roll gap, the greater the effect of roll crossing on the roll-gap asymmetry. Heavy mills should give more attention to factors or phenomena that is caused by roll crossing, such as the liner wear of bearing chocks and mill housing, tremendous roll axial force, etc.

(4) To prevent the occurrence of serious roll crossing in a 5000-mm rolling mill, the following criteria are recommended: the sum of the clearance and wear extent between the liners of both bearing chocks and mill housing in both the working and driving side is less than 9 mm.

Acknowledgments

The financial support of the Shanxi Province Natural Science Foundation Research Program(Grant No. 202203021222121), the Shanxi "1331Project" Key Innovative Research Team Fund, the Open Project of Research Institute of Hai'an-Taiyuan University of Technology (Grant No. 2023HA-TYUTKFYF008), the Chinese Postdoctoral Science Foundation (Grant No. 2021M702544), the School Fund of Taiyuan University of Technology (Grant No. 2022QN007), and the Shanxi Province Major Project of Science and Technology(Grant No. 20181102016) are gratefully acknowledged.

Author contributions

Xiaoxin Ma: Investigation, Formal analysis, Original draft writing, Programming; Peisen Yuan: Original draft writing, Programming, Editing; Fuyi Li: Editing, Review; Jiang Ji: Supervision, Review.

Declaration of competing interest

The authors declare that they have no known competing financial interests or personal relationships that could have appeared to influence the work reported in this paper.

Data availability statement

Almost all data generated or analyzed during this study are included in this published article. The other information or parameters used and/or analyzed during the current study are available from the corresponding author on reasonable request.

6 REFERENCES

[1] S. Omori, T. Kajiwara, H. Hino, H. Goto, Analysis of rolling load generated by pair crossing rolling mill, Ironmak. Steelmak., 31 (**2013**) 1, 71–80, doi:10.1179/030192304225012088

[2] J. G. Ding, Y. H. C. He, M. X. Song, Z. J. Jiao, W. Peng, Roll crown control capacity of sextic CVC work roll curves in plate rolling process, Int. J. Adv. Manuf. Technol., 113 (**2021**), 87–97, doi:10.1007/s00170-020-06536-8

[3] J. G. Cao, S. J. Liu, J. Zhang, P. Song, T. L. Yan, Y. Z. Zhou, ASR work roll shifting strategy for schedule-free rolling in hot wide strip mills, J. Mater. Process. Technol., 211 (**2011**) 11, 1768–1775, doi:10.1016/j.jmatprotec.2011.05.025

[4] X. B. Ma, D. C. Wang, H. M. Liu, C.C. Wen, Y. Zhou, Large concave roll technology for hot rolled silicon steel, Ironmak. Steelmak., 45 (**2018**) 1, 66–75, doi:10.1080/03019233.2016.1240841

[5] A. R. He, J. Shao, W. Q. Sun C. L. Guan, X. Y. Shen, J. P. Zhang, Transverse thickness deviation control of non-oriented silicon steel during cold rolling, J. Mech. Eng., 47 (**2011**) 10, 25–30, doi:10.3901/jme.2011.10.025

[6] A. Seilinger, A. Mayrhofer, A. J. Kainz, SmartCrown - A new system for improved profile and flatness control in strip mills, Steel Times Int., 26 (**2002**) 10,11–12, doi:10.1051/metal/2003001

[7] H. N. He, J. Shao, X. C. Wang, Q. Yang, Y. Liu, D. Xu, Y. Z. Sun, Research and application of approximate rectangular section control technology in hot strip mills, J. Iron Steel Res. Int., 28 (**2021**) 3, 279–290, doi:10.1007/s42243-021-00558-6

[8] A. R. He, Q. Yang, X. L. Chen, L. Zhao, H. R. Dong, Y. Q. Xu, Development and application of linearly variable crown work roll in hot strip mills, J. Mech. Eng., 44 (2008) 11, 255–259, doi:10.3901/jme.2008.11.255

[9] G. M. Liu, H. S. Di, A. Chang, Z. Y. Hou, Discussion on design of CVC roll contour and its equivalent crown, J. Northeast. Univ., Nat. Sci., 29 (**2008**) 10, 1443–1446, https://xuebao.neu.edu.cn/natural/EN/Y2008/V29/I10/1443

[10] H. B. Li, J. Zhang, J. G. Cao, F. W. Cheng, W. D. Hu, Y. Zhang, Roll contour and strip profile control characteristics for quintic CVC work roll, J. Mech. Eng., 48 (**2012**) 12, 24–30, doi:10.3901/JME.2012.12.024

[11] F. Schausberger, A. Steinboeck, A. Kugi, Mathematical modeling of the contour evolution of heavy plates in hot rolling, Appl. Math. Model., 32 (**2015**) 15, 4534–4547, doi:10.1016/j.apm.2015.01.017

[12] B. L. Lu, Tandem rolling and its equivalent roll crown curve, Baosteel Technology, (**1995**) 02, 50–53

[13] B. L. Lu, G.W. Zheng, Single cross rolling and equivalent crown, Iron Steel, 35 (**2000**) 01, 32–34. doi:10.13228/j.boyuan.issn0449-749x.2000.01.011

[14] W. M. Li, Z. B. Liu, L. Y. Ni, Y. S. Long, Technological principle on shape control by single declining roller in asymmetrical PC rolling mill, J. Iron Steel Res., 14 (**2002**) 02, 13–17, doi:10.13228/j.boyuan.issn1001-0963.2002.02.004

[15] M. Abbaspour, A. Saboonchi, Work roll thermal expansion control in hot strip mill, Appl. Math. Model., 32 (**2008**) 12, 2652–2669, doi:10.1016/j.apm.2007.09.011

[16] R. Servin Castañeda, F. Equihua Guillen, R. Torres Gonzalez, I. A. Facundo Arzola, Development of simple equation for calculating average wear of hot strip mill work rolls, Ironmak. Steelmak., 41 (**2014**) 5, 369–376, doi:10.1179/1743281213Y.0000000162

[17] S. M. Hwang, C. G. Sun, S. R. Ryoo, W. J. Kwak, An integrated FE process model for precision analysis of thermo-mechanical behaviors of rolls and strip in hot strip rolling, Comput. Method Appl. Mech. Eng., 191 (**2002**) 37, 4015–4033, doi:10.1016/S0045-7825(02)00298-0

[18] X. D. Wang, Q. Yang, A. R. He, R. Z. Wang, Comprehensive contour prediction model of work roll used in online strip shape control model during hot rolling, Ironmak. Steelmak., 34 (**2007**) 4, 303–311, doi:10.1179/174328107X168011

[19] Z. F. Chen, Theoretical and experimental research on roll of four-high strip mill, Doctor Dissertation, Shanghai Jiao Tong University, Shanghai, China, 2003

[20] X. D. Shu, G. X. Shen, The test of work roll axial force about 2350 aluminium foil mill and the shorter longevity analysis of end thrust bearing, Metall. Equip., 129 (**2001**) 5, 1–5

[21] G. X. Shen, M. Li, R. Shi, J. Yanagimoto, Indeterminacy of the offset mechanism and microscale static determinacy of roll system in four-high mill, J. Mech. Eng., 46 (**2010**) 10, 69–74, doi:10.3901/JME.2010.10.069

[22] G. X. Shen, Y. J. Zheng, M. Li, Development of statically determinate plate rolling mills that maintain the rolls parallel, J. Manuf. Sci. Eng., 135 (**2013**) 3, 922–926, doi:10.1115/1.4024039

[23] G. X. Shen, M. Li, Statically determinate characteristics of microdisplacement in a four-high mill, J. Mater. Process. Technol., 209 (**2009**) 11, 5002–5007, doi:10.1016/j.jmatprotec.2009.01.023

[24] T. Kiefer, A. Kugi, An analytical approach for modelling asymmetrical hot rolling of heavy plates, Math. Comp. Model. Dyn. Systems, 14 (**2008**) 14, 249–267, doi:10.1080/13873950701844915

[25] X. Liu, X. H. Liu, M. Song, L. Z. Liu, Theoretical analysis of minimum metal foil thickness achievable by asymmetric rolling with fixed identical roll diameters, Trans. Nonferrous Met. Soc. China, 26 (**2016**) 2, 501–507, doi:10.1016/S1003-6326(16)64138-9

[26] J. J. Minton, C. J. Cawthorn, E. J. Brambley, Asymptotic analysis of asymmetric thin sheet rolling, Int. J. Mech. Sci., 113 (**2016**), 36–48, doi:10.1016/j.ijmecsci.2016.03.024

[27] X. B. Ma, H. M. Liu, J. L. Sun, Z. Z. Zhang, Screw-down load deviation model of 5m heavy plate mill based on influence of back-up roll axial force, Ironmak. Steelmak., 43 (**2016**) 2, 112–120, doi:10.1179/1743281215Y.0000000055

[28] X. H. Zhou, J. X. Zhao, T. D. Lu, Transforming between spatial rectilinear coordinate system and non-linear coordinate system, Beijing Surv. and Mapp., (**2005**) 1, 33–35. doi:10.19580/j.cnki. 1007-3000.2005.01.010

[29] X. B. Ma, H. M. Liu, J. L. Sun, Z. Z. Zhang, S. W. Chen. Impact of main drive system of 5 m wide and heavy plate mill on screw-down load deviation, Eng. Failure Anal., 79 (**2017**), 913–927, doi:10.1016/j.engfailanal.2017.06.009